The effect of disorder of small spheres on the photonic properties of the inverse binary NaCl-like structure

IOP Publishing Journal of Physics: Condensed Matter
J. Phys.: Condens. Matter **29** (2017) 385101 (7pp) https://doi.org/10.1088/1361-648X/aa7ea9

The effect of disorder of small spheres on the photonic properties of the inverse binary NaCl-like structure

Harini Pattabhiraman and Marjolein Dijkstra

Soft Condensed Matter, Debye Institute for Nanomaterials Science, Department of Physics, Utrecht University, Princetonplein 5, 3584 CC Utrecht, Netherlands

E-mail: h.pattabhiraman@uu.nl and m.dijkstra@uu.nl

Received 31 May 2017, revised 1 July 2017
Accepted for publication 10 July 2017
Published 17 August 2017

Abstract

Inverse opal structures are experimentally realisable photonic band gap materials. They suffer from the drawback of possessing band gaps that are extremely susceptible to structural disorders. A binary colloidal NaCl lattice, which is also experimentally realisable, is a promising alternative to these opals. In this work, we systematically analyse the effect of structural disorder of the small spheres on the photonic properties of an inverse binary NaCl lattice with a size ratio of 0.30 between the small and large spheres. The types of structural disorders studied include the position of the small spheres in the octahedral void of the large spheres, polydispersity in size of the small spheres, and the fraction of small spheres in the crystal. We find a low susceptibility of the band gap of the inverse NaCl lattice to the disorder of the small spheres.

Keywords: colloids, photonic crystal, self-assembly

(Some figures may appear in colour only in the online journal)

1. Introduction

Photonic band gap (PBG) materials are structures in which the refractive index varies periodically in space on a length scale comparable to the wavelength of light. Similar to the way the motion of electrons is affected by the atomic lattice of a semiconductor, photons can be scattered multiple times by the photonic structure thereby resulting in either propagation or blocking of specific wavelengths of light through this structure. In case that the propagation of bands of wavelengths of light is disallowed for all directions and polarizations, the photonic crystal exhibits a photonic band gap [1, 2]. Three-dimensional photonic crystals with band gaps in the wavelengths pertaining to the visible and near-infra-red regions [3, 4] are believed to be the future of optical devices [5, 6], for which inverse opal structures are promising candidates. Although the research focus in recent years has shifted towards two-dimensional photonic crystals as they are easier to fabricate, interest in fabrication of three-dimensional photonic crystals such as the woodpile lattice seems to be on the rise [5, 7, 8].

Inverse opal structures consist of spheres made of a low dielectric contrast material embedded at the positions of a face-centered cubic (FCC) lattice inside a material with a high dielectric contrast. For instance an FCC structure of air spheres in silicon has a band gap between bands 8 and 9 with a relative gap width of 5% [9–11]. Reports of experimental realisations of these structures starting from a precursor colloidal FCC crystal are abundant [12–18]. The inverse crystal can be achieved from the colloidal crystal by infiltrating a high refractive-index dielectric material and then removing the solid spheres by etching or burning to create the air pockets [12]. However, the popularity of these FCC structures is damped by the fact that the photonic band gap formed in such structures is extremely fragile and highly susceptible to variations in position and size of the spheres [19, 20]. This imposes a strict restriction on the uniformity of these structures. Though there have been efforts to increase the band gap either by connecting the air spheres by cylindrical tunnels [21] or by creating voids by incomplete infiltration of a high dielectric contrast material [3], such increments do not give any warranty against the

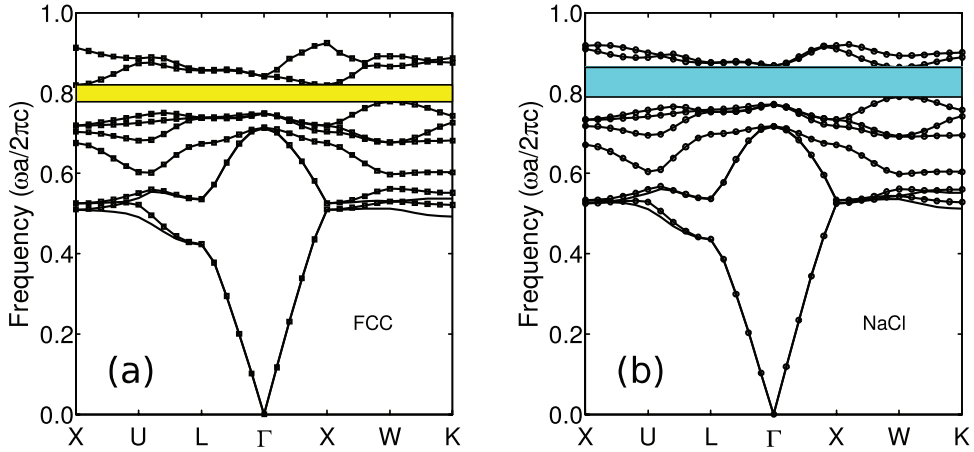

Figure 1. Comparison of photonic band structures of (a) a face-centered cubic (FCC), and (b) a NaCl lattice of air spheres ($\epsilon = 1$) in silicon ($\epsilon = 12$). The large spheres in both the structures have a close-packed configuration. In the NaCl structure, the spheres have a size ratio of $q = r_s/r_l = 0.3$, where r_s and r_l are, respectively, the radius of the small and large spheres. The band gap in the FCC and NaCl structures are, respectively, coloured in yellow and cyan. The reduced frequency is written as $\omega^* = \omega a/2\pi c$.

destruction of the photonic band gap in these photonic band gap materials. Another possible route is to embed a different material to the existing dielectric structure such as graphene [22, 23]. A more attractive solution stems from the reported increase in the photonic band gap of two-dimensional photonic crystals of dielectric rods in a square, triangular or honeycomb lattice by the addition of smaller interstitial rods [24, 25]. This increase in the gap width is due to the increase in the filling fraction of the dielectric without a disruption in the connectivity of the lattice. Analogously, doping the octahedral interstices of the FCC lattice leads to a binary NaCl lattice, which in its inverse form is reported to possess a band gap with a relative gap width of 9% [26, 27]. A comparison between the band structures calculated for the close-packed inverse FCC and NaCl structures is given in figure 1. From the figure, we note (1) the larger band gap in NaCl in comparison to the FCC structure and (2) the position of the gap in NaCl is a little higher than in FCC. However, the question regarding susceptibility of this NaCl-like structure to disorder is, as yet, not investigated.

To answer this question, we first need to understand the construction of the NaCl lattice and consider the different kinds of disorder that are formed in this structure during its experimental fabrication. The binary NaCl structure consists of spheres of two different sizes, where each species is ordered on a FCC lattice. This inter-penetration of two FCC lattices results in a scenario where the small spheres are positioned in the octahedral voids of the FCC lattice of the large spheres. For a close-packed FCC lattice of large spheres with a radius r_l, the corresponding radius of the small spheres r_s should lie between the radius of the tetrahedral ($r_{te} = 0.22r_l$) and the octahedral ($r_{oc} = 0.41r_l$) voids. Large binary colloidal crystals with a NaCl structure have been fabricated using hard-sphere-like silica spheres with a size ratio $q = r_s/r_l = 0.30$ [28]. At this size ratio, the small spheres are not in contact with the large spheres and in principle, can rattle inside the octahedral void. Thus, when the structure is inverted, the position of the small spheres may not be in the centre of the void. We also note that for this size ratio the small spheres do not fit in the tetrahedral voids. Furthermore, a size polydispersity of about 2% for the large and 7% for the small spheres was reported during the fabrication. Accordingly, the first two parts of this work is concerned with the study of the effect of positional disorder and size polydispersity of the small spheres on the photonic properties of a binary colloidal NaCl lattice.

In the third part of this work, we address the question of how the photonic properties change for these binary structures upon changing the number fraction of small spheres, i.e. by varying the compositions in between those of the FCC and the NaCl structures, both of which possess a photonic band gap. This is particularly interesting because of the following reasons: (1) It was recently demonstrated that the so-called interstitial solid solution (ISS) is thermodynamically stable in a binary hard-sphere mixture with a size ratio $q = 0.30$. The ISSs in this binary system consists of a FCC of large spheres but with only a fraction of the octahedral holes filled with small spheres [29]. (2) ISSs of varying compositions can be formed by sedimentation experiments in which the fraction of small spheres decreases along the height of the sedimentation column [27]. (3) ISSs have a huge effect on the photonic properties of the parent material as demonstrated by the change in the structural colour of FCC photonic colloidal crystals upon interstitially doping with spherical nanoparticles [30]. Thus, in this work, we also study the effect of small sphere composition on the photonic properties of a binary colloidal ISS with the spheres positioned on an NaCl lattice.

We wish to point out here that although one might expect that the structural disorder of the large spheres has a larger effect on the band gap, we exclusively focus this work on the disorder of the small spheres. This is because of the following reasons: Firstly, we expect the effect of the disorder of the large spheres in the NaCl lattice to be similar to that of the FCC, but less pronounced due to (1) the larger band gap width of the NaCl lattice, and (2) the fact that the small spheres in the NaCl lattice will constrain the movement of the large spheres. We will briefly explain these here. According to (1), for a FCC lattice, a band gap width of about 5% was nullified with randomness in the position and size of large

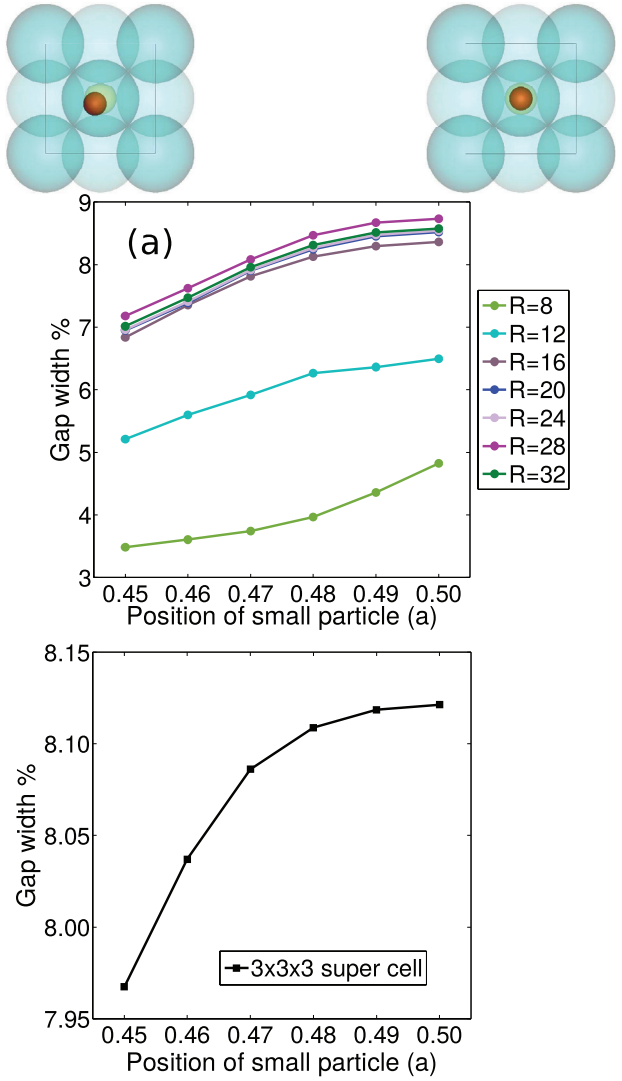

Figure 2. Relative gap width of a NaCl lattice of air spheres ($\epsilon = 1$) in silicon ($\epsilon = 12$) with a size ratio of $q = r_s/r_l = 0.3$ as a function of the positional coordinate of a small sphere (in units of the lattice constant a) for (a) an unit cell calculated at different resolutions R, and (b) a super cell of size $3 \times 3 \times 3$ and resolution $R = 24$. The positional extremities are shown in the schematic representations on the top. We represent a single small sphere (red) in an octahedral void (green) surrounded by the large spheres (blue).

spheres with a range less than 2% of the lattice constant [19, 20]. However, as previously mentioned, the band gap width of a NaCl lattice is almost twice as large as that of the FCC lattice consisting of the same dielectric material. Thus, contrary to the situation of increasing the band gap by using a material with higher dielectric constant [19, 20], this could mean that the NaCl lattice can withstand disorders of larger magnitude than the FCC. The situation presented in (2) means that the possible range of positional disorder of the large sphere in a NaCl lattice is limited because of the presence of the small spheres in between them. This, also reduces the effect of the positional disorder of the large spheres. Secondly, during the fabrication of these crystals by sedimentation, the position and composition of the small spheres are more prone to vary in comparison to that of the large spheres and it is thus important to investigate the effect of disorder of the small spheres. However, we have not come across such a study. Our present work is a step in this direction. This paper is organised as follows. We present the method used to calculate the photonic band structures in section 2. We then individually discuss our method for studying each of the three types of disorders, and evaluate the effect on the photonic properties of the binary NaCl-like structure in section 3. We end with some conclusions in section 4.

2. Methods

We study the effect of positional disorder, size polydispersity and composition of the small spheres on the photonic properties of a binary colloidal NaCl-like structure by calculating the photonic band structure diagrams. We focus here on the inverse structures composed of air spheres with dielectric constant $\epsilon = 1$ in silicon with $\epsilon = 12$.

We calculate the photonic band structure diagrams using the open-source 'MIT Photonic-Bands' software package [31]. This software package computes fully-vectorial eigenmodes of Maxwell's equations with periodic boundary conditions by preconditioned conjugate-gradient minimisation of the block Rayleigh quotient in a plane wave basis [31]. We describe a primitive cubic NaCl unit cell of lattice constant a by a large sphere with radius $r_l = 0.35\,350a$, and small sphere with radius $r_s = 0.10\,605a$. This results in a NaCl-like structure with a volume fraction $\left(\eta = 4/3\left(N_l\pi r_l^3 + N_s\pi r_s^3\right)/V\right)$ of 0.76 and a size ratio of $q = r_s/r_l = 0.30$. For comparison, we mention that the volume fraction of a close-packed FCC lattice is 0.74; while the maximum packing of an NaCl lattice is obtained at a size ratio $q = 0.41$ and is equal to 0.79. In this primitive representation of the unit cell, the large sphere is positioned at the origin and the small sphere at $(0.50a, 0.50a, 0.50a)$. We normalise each parameter with respect to the lattice constant a. Thus, the band structures can be tuned to any length scale by scaling with a. In order to study the various defects, we make use of a super cell approximation, in which a large crystal with a defect is placed in a super cell and then repeated periodically in a three-dimensional space. We use a super cell containing $3 \times 3 \times 3$ unit cells. We wish to point out here that the size of the super cell is relatively small compared to the system size used in experiments. So, these super cells can be considered as a periodic representation of the disorder. Because of memory constraints experienced in running these simulations, different mesh resolutions were used for studying the different aspects of disorder. The resolution cubed equals the number of plane waves included in the calculations, which is equal to the number of grid points used to discretise the unit cell or super cell.

3. Results and discussion

In this section, we individually present the results pertaining to each of the three types of disorder.

3.1. Effect of positional disorder of the small spheres

First, let us take a look at the effect of the position of the small sphere in the octahedral void. To assess this, we consider lattices in which the position of the small sphere varies from the centre to the periphery of the octahedral void. All three coordinates of the small sphere in a unit cell are collectively changed from $(0.50a, 0.50a, 0.50a)$ to $(0.45a, 0.45a, 0.45a)$ in steps of $0.01a$. We do not change the coordinate of the sphere in a single dimension with respect to the other two. We perform this study using both a unit cell and a super cell. We state here again in the unit cell simulations, we consider a primitive unit cell consisting of one large and one small sphere. On the other hand, the $3 \times 3 \times 3$ super cell consists of a total of 27 large and 27 small spheres. In the case of the unit cell, the positional change denotes a collective change in the entire lattice due to periodic boundary conditions. On the other hand, in the case of the super cell, we only vary the position of the central sphere while keeping the position of the other 26 spheres intact. We perform photonic band gap calculations on the unit cell using resolutions varying from 4 to 32 to obtain an indication regarding the resolution to be used in the super cell calculations. On the basis of these results, we decide to use a super cell with a resolution of 24. We compare the various band gaps obtained in each case by calculating the relative gap width, i.e. the ratio of the gap width and the mid-gap frequency.

We plot the relative gap width as a function of the positional coordinate in figure 2. On the top of the figure, we show schematic representations of the extreme positions of the small sphere (red) in the octahedral void (green). The surrounding large spheres (blue) are also shown. Figure 2(a) deals with the calculations performed on a unit cell, while figure 2(b) shows that of the super cell. We make four observations from this figure. Firstly, in figure 2(a), we see that the gap width starts to converge at a resolution of 16. This is the lowest resolution that can be used in the super cell calculations. Further, in a study of the band gap as a function of the resolution for the ideal NaCl-like structure (not given here), we find that the band gap width at resolutions $32 \leqslant R \leqslant 60$ is 8.18 ± 0.07. The band gap calculated at $R = 24$ is 8.12, which falls within the above mentioned range. Thus, our resolution value of 24 is justified. Secondly, we observe that the gap width calculated for the ideal NaCl lattice, i.e. at $(0.50a, 0.50a, 0.50a)$, is slightly different in the case of the unit cell (figure 2(a)) and the super cell (figure 2(b)). We attribute this difference to the different mesh resolutions used to discretise the unit cell and super cell. Thirdly, we find that the presence of a photonic band gap is independent of the position of the small sphere, but the relative band gap width decreases with a larger deviation of the small sphere from its ideal position. This is due to the structural disorder that is introduced by the eccentric movement of the small sphere. Lastly, we observe that, at the highest reported resolution for the unit cell, the reduction in the relative gap width is close to two percentage points (around 22%) when the sphere is moved from the centre to the periphery of the octahedral void. In contrast, the corresponding reduction in case of the super cell is about 0.15 percentage points (about 2%). This is expected because in the case of the super cell, we calculate the effect of the movement of only a single small sphere; while in the case of the unit cell all small spheres in the system are effectively moved.

3.2. Effect of size polydispersity of the small spheres

We study the effect of size polydispersity of the small spheres by changing the radius of a single sphere in a super cell, termed as 'defect' particle. We do not, however, change the size of the large spheres, and all particles are kept fixed on their ideal lattice positions. In general, changing the size of the defect sphere results in the addition or removal of dielectric material from the structure and this results in the formation of degenerate states inside the band gap in case of single-component structures [32]. Reducing the size of the dielectric spheres from the ideal radius to zero results in moving the defect state from the lower end to the middle of the band gap. Increasing the size of the dielectric spheres would have an opposite effect; i.e. the defect state moves from the upper end to the lower end of the band gap [32]. However, the behaviour obtained by changing the size of one component with respect to the other in a binary system is not so straightforward. Practically, one would expect polydispersity to be manifested as a random configuration of small particles of different sizes. Our study, where we consider only a single defect per super cell, is a starting point towards this. In our case, we obtain a periodic repetition of the defect.

Here, we vary the radius of the defect sphere r_d in the calculations from 0.00 to $0.15a$ in steps of $0.01a$. For the analysis, we normalise the defect radius with the ideal radius of the large sphere $r_d^* = r_d/r_l$. The normalised defect radius then varies from 0.00 to 0.42. With this variation, we span the size spectrum from a vacancy to a sphere slightly larger than the radius of the octahedral void, $r_{ov} = 0.41r_l$. This enables us to calculate both the effect of decreasing as well as increasing the radius of the air sphere. For these calculations, due to memory constraints of our computing cluster, we use a super cell of resolution 16. The results are given in figure 3. We find that the resulting behaviour is different for $r_d^* < 0.37$ and $0.37 \leqslant r_d^* \leqslant 0.42$. The formation of defect states inside the band gap occurs only at larger defect sizes, i.e. $0.37 \leqslant r_d^* \leqslant 0.42$. Let us look at these two situations separately. In figure 3(a), we plot the variation of the gap width as a function of the defect size r_d^*. We find that the gap width decreases upon increasing the defect size. This results in an interesting scenario where the presence of a vacancy in the crystal ($r_d^* = 0.00$) has a larger gap width than the ideal NaCl lattice ($r_d^* = 0.30$). This hints that the presence of a small fraction of vacancies in the crystal may in fact be beneficial for its photonic properties. A more detailed study of these vacancies (composition) will be presented in the next section. As mentioned, for $0.37 \leqslant r_d^* \leqslant 0.42$, we find the formation of defect states in the photonic band gap as shown in figure 3(b). We make the following three observations. Firstly, we notice the presence of three degenerate defect states at each defect size. Such defects can act as a small-sized optical

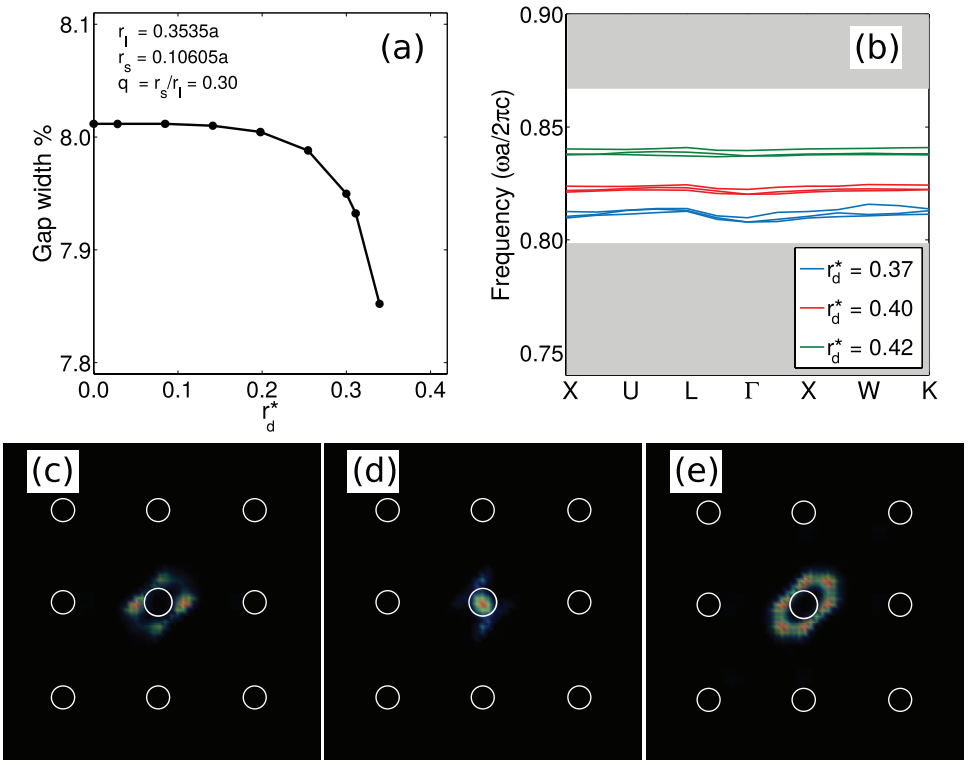

Figure 3. Effect of the size of a small sphere on the photonic properties of an NaCl lattice of air spheres ($\epsilon = 1$) in silicon ($\epsilon = 12$) with a size ratio of $q = r_s/r_l = 0.3$ calculated by changing the radius $r_d^* = r_d/r_l$ of a single sphere in a super cell of size $3 \times 3 \times 3$: (a) Variation in gap width, in %, as a function of radius of the small defect sphere for $r_d^* < 0.37$. (b) Frequency of defect states obtained for $0.37 \leqslant r_d^* \leqslant 0.42$. The shaded regions indicate the edges of the band gap. ((c)–(e)) Electric-field distribution of the resonant modes of the three degenerate defect states at $r_d^* = 0.37$. The open circles represent the position of the small spheres and the defect sphere is at the centre.

resonator. Secondly, we note that these defect bands are not flat. One would expect a flat defect band for a point defect in an infinite structure [33]. The optical coupling between the different super cells results in these non-flat curves. Thirdly, we observe that the frequency of the defect state increases with increasing defect size. This behaviour is similar to that in a single-component system as described above [32]. In figures 3((c)–(e)), we plot the distribution of the electric field across the sample in the defect states obtained at $r_d^* = 0.37$. The open circles represent the position of the small spheres and the defect sphere is at the centre. We see that the resonant modes of the electric field are localised in the vicinity of the defect, thereby resembling a microcavity. Such a microcavity can be used to enhance the rate of spontaneous emission of a photonic crystal [32]. We note that each defect state is split into three because of the difference in alignment of the defect field with respect to the underlying lattice. Furthermore, the presence of a threshold (in terms of the defect size) for the formation of defect states agrees well with the localisation theory in three dimensions, i.e. a certain critical degree of disorder is required for localisation [34, 35].

3.3. Effect of composition of the small spheres

Finally we study the effect of composition of the binary mixture on the photonic properties. In other words, we study the photonic properties of the interstitial solid solutions with compositions of small spheres intermediate to the FCC and NaCl compositions. At compositions closer to NaCl, this also serves as a study on the effect of vacancies. To this end, we begin with a super cell of FCC and add small spheres in steps of three to it, i.e. from 0 to 27 small spheres in a $3 \times 3 \times 3$ super cell. In the case of 27 small spheres, the system reduces to the NaCl-like structure. At each composition, we use three random configurations of small spheres. These calculations were performed at a resolution of 24.

To analyse this, we plot the relative gap width and the gap map as a function of composition in figure 4. We represent the composition as the number ratio of small spheres to all spheres in the system, $x_s = N_s/(N_s + N_l)$, where N_s and N_l are respectively the number of small and large spheres in the system. A value of $x_s = 0$ represents a pure FCC lattice, while $x_s = 0.5$ is the NaCl lattice. In figure 4(a), we plot the variation of the gap width as a function of composition. The black dots are the gap width obtained at each of the three configurations used at each composition and the blue curve connects the average of these three values. The behaviour in this plot can be summarised in the following four observations: (1) A continuous curve from $x_s = 0.0$ to 0.5 indicates that the ISS possesses a photonic band gap throughout the entire range of compositions. (2) The band gap increases gradually till $x_s = 0.4$ after which we see a sudden increase in the gap width. This could be due to the filling of most of the octahedral voids and thus, a reduction in the randomness of the structure. (3) The scatter in the

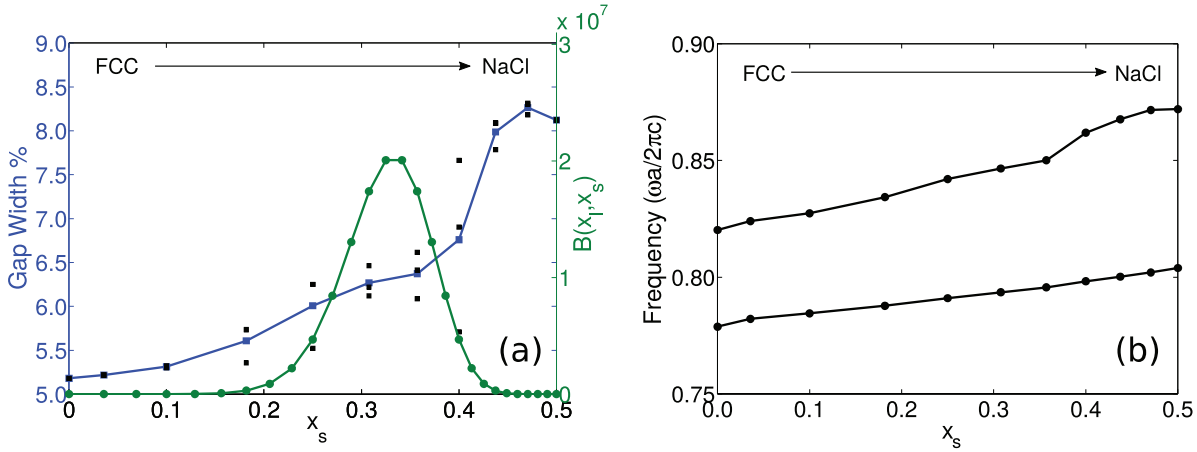

Figure 4. Photonic properties of the interstitial solid solution (ISS) with compositions between those of the FCC and NaCl lattices: Variation of (a) band gap width, and (b) position of the edges of the band gap as a function of composition ($x_s = N_s/(N_s + N_l)$) when going from an inverse FCC to a binary NaCl lattice of air spheres ($\epsilon = 1$) in silicon ($\epsilon = 12$) with a size ratio of $q = r_s/r_l = 0.3$ calculated using a super cell of size $3 \times 3 \times 3$. N_s and N_l are, respectively, the number of small and large spheres in the system. In (a), the black dots are the individual values obtained for each of the three configurations used at each composition and the blue curve connects the average of the three values. Here, we also plot a binomial distribution of the number of ways the small spheres can be arranged on the sub-lattice of an NaCl-like structure in green. In (b), the curve is drawn for the average of the three typical configurations.

gap widths calculated for the various configurations at intermediate compositions is higher than in the extremes. This can be explained by plotting the binomial distribution representing the number of ways the small spheres can be arranged, shown as the green curve in figure 4(a). We notice a direct correlation between the scatter in the gap width and the binomial distribution indicating that the sampling size used at the intermediate compositions may be inadequate. (4) At compositions close to $x_s = 0.50$, we find a small increase in the gap width as reported in the previous section. This reinforces the advantageous effect of the presence of a small concentration of vacancies in the crystal. Correspondingly, we plot the gap map with the position of the band gap as a function of composition in figure 4(b) using the average of the three values. We observe a similar continuous increase from the FCC to the NaCl gap positions, that agrees well with the band structure shown in figure 1.

4. Conclusions

In conclusion, we have studied the effect of various disorders pertaining to the small spheres on the photonic properties of a binary NaCl lattice consisting of air spheres in silicon at a size ratio $q = r_s/r_l = 0.30$. Firstly, we confirm that the inverse NaCl-like structure has a larger band gap than the inverse FCC structure. We then find that the photonic band gap in the inverse NaCl is not very susceptible to disorder in terms of randomness in sphere position, size, and composition of the small particle. We find that the NaCl possess a band gap irrespective of the position of the small sphere inside the octahedral void. However, the relative gap width decreases with larger deviation from its ideal position. Additionally, we find interesting effects of the size polydispersity of the small sphere. We find an increase in the relative band gap width of about 0.15 percentage points (about 19%) for up to 70% reduction in the radius of the small particle, i.e. reducing the defect radius r_d from $0.3r_l$ to $0.2r_l$. Furthermore, for a particle radius larger than the ideal size of the small particles, we find the formation of microcavities with resonant states inside the band gap. It is worth pointing out that we find that the presence of up to 10% vacancies in small spheres does not greatly influence the band gap of the NaCl lattice. Our results, thus, show that the NaCl-like structure has a low susceptibility to structural defects of the small spheres.

Acknowledgments

This work is part of the Industrial Partnership Programme 'Computational Sciences for Energy Research' (12CSER004) of the Foundation for Fundamental Research on Matter (FOM), which is part of the Netherlands Organisation for Scientific Research (NWO). This research programme is co-financed by Shell Global Solutions International B V. We thank Sergei Sokolov and Guido Avvisati for critical reading of this manuscript.

ORCID iDs

Harini Pattabhiraman https://orcid.org/0000-0001-5770-9190

References

[1] John S 1987 *Phys. Rev. Lett.* **58** 2486
[2] Yablonovitch E 1987 *Phys. Rev. Lett.* **58** 2059
[3] Busch K and John S 1998 *Phys. Rev.* E **58** 3896
[4] Hynninen A P, Thijssen J H J, Vermolen E C M, Dijkstra M and van Blaaderen A 2007 *Nat. Mater.* **6** 202
[5] Noda S, Tomoda K and Yamamoto N 2000 *Science* **289** 604
[6] Han H, Vijayalakshmi S, Lan A, Iqbal Z, Grebel H, Lalanne E and Johnson A M 2003 *Appl. Phys. Lett.* **82** 1458
[7] Van den Broek J, Woldering L, Tjerkstra R, Segerink F, Setija I and Vos W 2012 *Adv. Funct. Mater.* **22** 25

[8] Frölich A, Fischer J, Zebrowski T, Busch K and Wegener M 2013 *Adv. Mater.* **25** 3588
[9] Yablonovitch E and Gmitter T J 1989 *Phys. Rev. Lett.* **63** 1950
[10] Sözuer H S, Haus J W and Inguva R 1992 *Phys. Rev.* B **45** 13962
[11] Moroz A and Sommers C 1999 *J. Phys.: Condens. Matter* **11** 997
[12] Wijnhoven J E G J and Vos W L 1998 *Science* **281** 802
[13] Vlasov Y A, Bo X Z, Sturm J C and Norris D J 2001 *Nature* **414** 289
[14] Schroden R C, Al-Daous M, Blanford C F and Stein A 2002 *Chem. Mater.* **14** 3305
[15] Qi M, Lidorikis E, Rakich P T, Johnson S G, Joannopoulos J D, Ippen E P and Smith H I 2004 *Nature* **429** 538
[16] Jun Y, Leatherdale C A and Norris D J 2005 *Adv. Mater.* **17** 1908
[17] Liu Y, Wang S, Lee J W and Kotov N A 2005 *Chem. Mater.* **17** 4918
[18] Stein A, Wilson B E and Rudisill S G 2013 *Chem. Soc. Rev.* **42** 2763
[19] Li Z Y and Zhang Z Q 2000 *Phys. Rev.* B **62** 1516
[20] Li Z Y and Zhang Z Q 2001 *Adv. Mater.* **13** 433
[21] Doosje M, Hoenders B J and Knoester J 2000 *J. Opt. Soc. Am.* B **17** 600
[22] Kaipa C S, Yakovlev A B, Hanson G W, Padooru Y R, Medina F and Mesa F 2012 *Phys. Rev.* B **85** 245407
[23] Fan Y, Wei Z, Li H, Chen H and Soukoulis C M 2013 *Phys. Rev.* B **88** 241403
[24] Anderson C M and Giapis K P 1996 *Phys. Rev. Lett.* **77** 2949
[25] Broeng J, Barkou S E, Bjarklev A, Knight J C, Birks T A, St P and Russell J 1998 *Opt. Commun.* **156** 240
[26] Thijssen J 2007 Characterization of photonic colloidal crystals in real and reciprocal space *Thesis* Utrecht University
[27] Vermolen E C M 2008 Manipulation of colloidal crystallization *Thesis* Utrecht University
[28] Vermolen E C M, Kuijk A, Filion L C, Hermes M, Thijssen J H J, Dijkstra M and Van B A 2009 *Proc. Natl Acad. Sci. USA* **106** 16063
[29] Filion L, Hermes M, Ni R, Vermolen E C M, Kuijk A, Christova C G, Stiefelhagen J C P, Vissers T, Van Blaaderen A and Dijkstra M 2011 *Phys. Rev. Lett.* **107** 168302
[30] Pursiainen O L, Baumberg J J, Winkler H, Viel B, Spahn P and Ruhl T 2007 *Opt. Express* **15** 9553
[31] Johnson S and Joannopoulos J 2001 *Opt. Express* **8** 173
[32] Villeneuve P R, Fan S and Joannopoulos J D 1996 *Phys. Rev.* B **54** 7837
[33] Joannopoulos J D, Johnson S G, Winn J N and Meade R D 2011 *Photonic Crystals: Molding the Flow of Light* 2nd edn (Princeton, NJ: Princeton University Press)
[34] Wiersma D S, Bartolini P, Lagendijk A and Righini R 1997 *Nature* **390** 671
[35] Schwartz T, Bartal G, Fishman S and Segev M 2007 *Nature* **446** 52